Int. J. Solids Structures Vol. 24, No. 9, pp. 881–891, 1988
Printed in Great Britain.

0020-7683/88 $3.00+ .00

FINITE ELEMENT SIMULATION OF INDENTATION EXPERIMENTS

A. K. BHATTACHARYA
Department of Mechanical Engineering, Stanford University, Stanford, CA 94305, U.S.A.

and

W. D. NIX
Department of Materials Science and Engineering, Stanford Univesity, Stanford, CA 94305, U.S.A.

(*Received* 1 *October* 1987; *in revised form* 12 *February* 1988)

Abstract—Indentation experiments are now being used to study the elastic and plastic properties of materials on a sub-micrometer scale. Simulations of these experiments have been performed using the finite element method under the conditions of frictionless and completely adhesive contact and within the context of incremental elasto-plasticity. Comparison of these simulated results with experimental results demonstrates that the continuum based finite element approach has the capability to determine the load–depth response of a sub-micrometer indentation test. It is also shown that the hardness and elastic modulus of the material can be obtained from the loading and unloading portions of these simulated curves.

INTRODUCTION

In recent years various sophisticated thin film deposition techniques have been developed in response to demands for better materials for high technological applications, especially in miniaturized electronic components. These techniques, such as: sputtering, vapor deposition, ion implantation, laser glazing and other modern surface modification techniques, involve tailored control of the mechanical and structural properties of the material involved. With respect to mechanical properties, these kinds of control depend on a trial and error approach and little is known fundamentally about the relationships between the film stress, hardness, yield strength, elastic modulus and the film thickness. The present work contributes to the understanding of the sub-micrometer indentation tests that are now being used to study the mechanical properties of these important thin films.

For over four decades, indentation hardness testing has been effectively used to determine the strength of materials very near the surface of the material. Hardness measurements have been attractive because they can be made easily on a variety of materials. But, because of the comparatively large indentations involved, even traditional microhardness tests are not well suited for determining the properties of thin films with typical thicknesses in the range of a few hundred angstroms to just a few micrometers. At present, very low load microhardness testers[1–3], which produce indentation depths as small as a few hundred angstroms, represent the most successful technique for studying the mechanical properties of thin films. Although various fundamental mechanical properties appear to be obtainable from these tests, very little effort has been made to understand the mechanics of the plastic deformation involved in these sub-micrometer indentations. The lack of knowledge in this area makes it difficult to determine the relative merits of various modifications that are necessary for designing a typical thin film system. It is, therefore, important to conduct continuum mechanics analyses in an effort to understand the underlying mechanics of these indentation tests.

A few analytical treatments related to indentation mechanics exist in the literature. The solution for a flat ended circular punch contacting a half space is well known[4]. Elastic normal contact problems for layered media were analyzed by Chen and Engel[5] and analyses of some punch problems for thin films on substrates were also given by King[6]. All of these solutions are applicable to elastic deformation only and cannot be used to

predict the complex elastic–plastic deformation involved in a typical indentation test. A few investigators[7–10] have used the finite element technique to analyze large indentations typical of the Brinell hardness test. The same method has also been used to calculate stresses in contact situations[11]. Semi-empirical analyses for indentation problems have been provided by other investigators[12–14]. Except for the work of Bourcier *et al.*[7], no detailed analyses have been made for extremely small indentations, such as those produced in typical sub-micrometer hardness tests[1, 3]. Due to the obvious mathematical complexities involved in such analyses, the finite element method is required and has been used in this investigation. The analysis involves a simulation of indentation tests, from which insight into the various mechanical properties of thin films can be gained. This work represents the first part of a more extensive theoretical research program aimed at understanding the mechanical properties of thin films on substrates. In the present study, the goals have been : (a) to demonstrate the feasibility of modeling a typical hardness test using the finite element technique and (b) to show how relevant basic mechanical properties can be extracted from such simulated results.

THE FINITE ELEMENT MODEL

Sub-micrometer indentation testing permits the measurement of force–distance relations on a very small scale; a detailed description of this can be found elsewhere[1, 3]. Simulations of these force–distance relations for the indentation of nickel, silicon and aluminum using a rigid indenter were performed using the large strain elasto-plastic feature of the ABAQUS finite element code[17], with uniaxial stress–strain data as input. The quasi-nature of the process permits us to use the static analysis performed by the program. Underlying the approach in this code is the discretization of the continuum involved; the indenter was considered to be perfectly rigid. Also, an important feature of this program involves the capability to model contact between the indenter and the sample as a sliding interface. The initial nodal gaps between the indenter and the surface of the specimen were prescribed and the program automatically keeps track of their change and indicates any gap closure or opening in a particular direction. These interface elements thus simulate contact between the indenter and the specimen surface. Whenever the closure distance between the indenter and the specimen becomes zero, contact is assumed and an external reaction force is exerted on this material point to keep it moving along with the indenter. Because the program calls for incremental loading and also makes use of interface elements, the expanding contact area associated with indentation occurs naturally whenever new interface elements come into contact.

In this analysis, the indenter and specimen are treated as bodies of revolution to avoid the inherent three-dimensional nature of the problem of indentation with a pyramid shaped indenter. If a pyramid indenter was used, it would have an elastic singularity at its edges but this would affect only the stress–strain response of a few of the elements adjacent to these edges. Thus, it is not expected to cause any noticeable difference in the load–deflection response of the material. Although this approximation is considered to be acceptable for the case of continuum plasticity, a three-dimensional analysis would be needed to treat crystal plasticity. Thus, in the present treatment the pyramid indenter was approximated by an axisymmetric cone of equal volume for a given indenter depth. The indenter and the specimen are shown schematically in Fig. 1, along with the appropriate boundary conditions for the problem. Symmetry properties have been used to simplify the boundary conditions. During preliminary simulations the boundary condition on the surface on the right-hand side of the specimen was changed from fixed radial displacements to traction free; this change had no effect on the indentation parameters, thus showing that this boundary was indeed remote. Because very small indentations were being simulated, the meshes near the indenter needed to be very fine to be able to describe the deformation and stress gradients associated with indentation with sufficient accuracy. Thus, extremely fine mesh sizes were used under the indenter; they became progressively coarser at distances farther away from the indenter. Axisymmetric four node elements were used for the continuum. In order to obtain an accurate estimate of the radius of the contact area, an extremely fine mesh

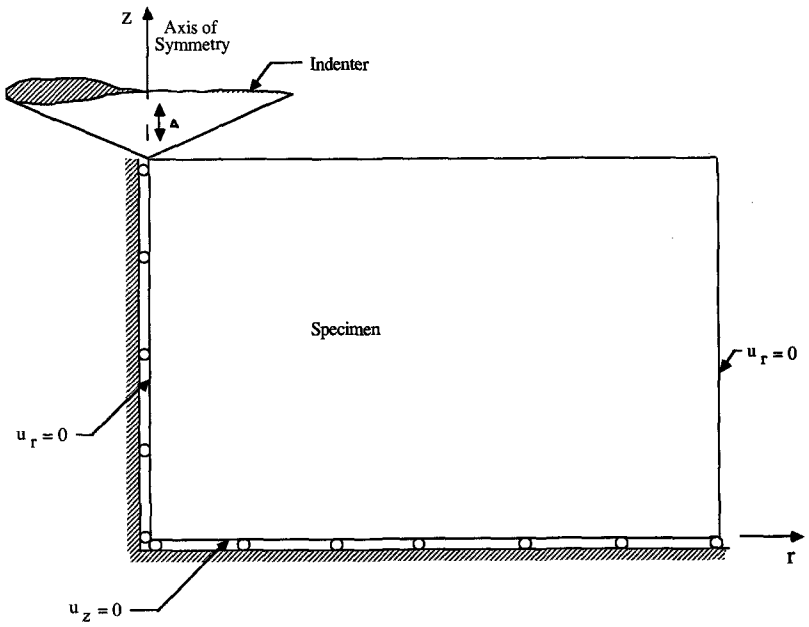

Fig. 1. Schematics of the specimen under the indenter showing the boundary conditions.

thickness of the order of 0.02 μm had to be used along most of the indenter contact surface. To keep the computer time within limits, a total of 461 elements including the interface elements were used for representing the deformed material. Figure 2 represents a magnified view of the elements near the indenter and the staircase arrangement for the other elements at points farther away from the indenter. When two elements are connected to a single element in this distribution, the middle node on the common face is constrained to lie on a straight line defined by the two corresponding end nodes.

To simulate a typical indentation process, a downward displacement (negative z-direction in Fig. 1) was imposed on the indenter; this causes the indenter to push into the surface of the material. Subsequently, the indenter was given an upward displacement until

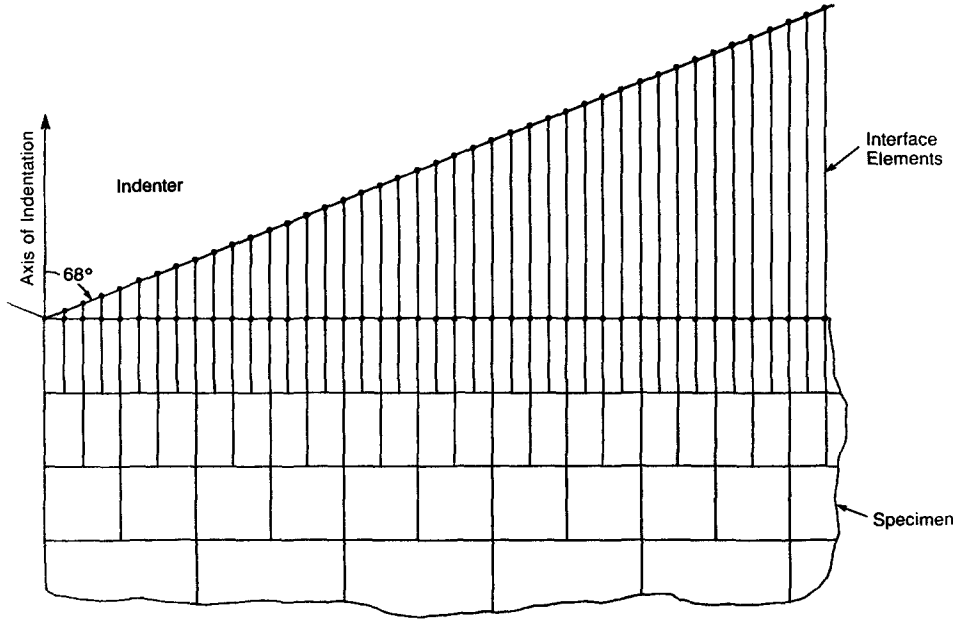

Fig. 2. Detailed pattern of mesh distribution near the indenter showing interface elements.

Table 1. Elastic and plastic properties of nickel, silicon and aluminum used in the analysis

Material	Young's modulus (GPa)	Poisson's ratio	Yield stress (MPa)	Strain hardening rate (MPa)
Nickel	207	0.31	350	380
Silicon	127	0.278	4410	0
Aluminum	75.9	0.33	485	146

it was free of contact with the specimen. For a given indenter displacement, the corresponding load determination was achieved by summing the reaction forces at the contact node points on the indenter. The interface between the specimen and the indenter was assumed to be frictionless since no noticeable change in the load–displacement response was observed by using a friction coefficient of 1. The mesh thickness of 0.02 μm along the indenter contact surface was determined by finding the mesh size below which no further significant changes in the indentation load–displacement response were observed. The hardness was also observed to remain constant with increasing indentation depth when the mesh was refined to this point (Figs 8 and 9).

The constitutive model for the specimen material (nickel, silicon and aluminum) was that of an elastic–plastic von Mises material with isotropic hardening. Two separate cases of strain hardening were considered, one with no strain hardening (i.e. the material was assumed to be elastic–fully plastic) and the other with a linear strain hardening rate of $\mu/200$ for the material under consideration. The material properties used in the calculations are given in Table 1. The finite element calculations were performed using an IBM 4341 mainframe computer with run times of 15–25 h for average indentation depths.

RESULTS AND DISCUSSION

Results of the load–displacement simulation are shown in Figs 3 and 4. In these plots comparison is made between the experimental data obtained by Pethica *et al.*[1] for pure nickel and silicon and the simulated response from finite element calculations. The material properties for these simulations are given in Table 1. The agreement between our finite element analysis and experimental results is satisfactory, thus indicating the feasibility of using finite element analysis to describe the sub-micrometer indentation process. Slight numerical oscillations present in the load–depth curves are caused by discontinuous contact of the test specimen nodal points with the indenter surface. The differences between the

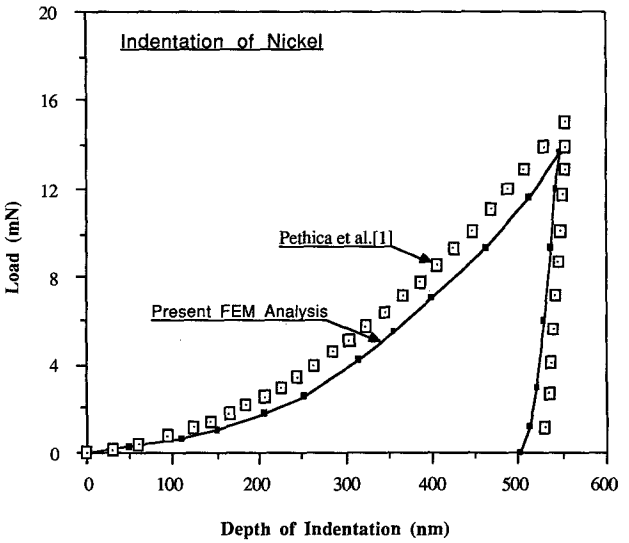

Fig. 3. Comparison between the results from the present FEM analysis and those from Pethica *et al.*[1] on indentation of nickel.

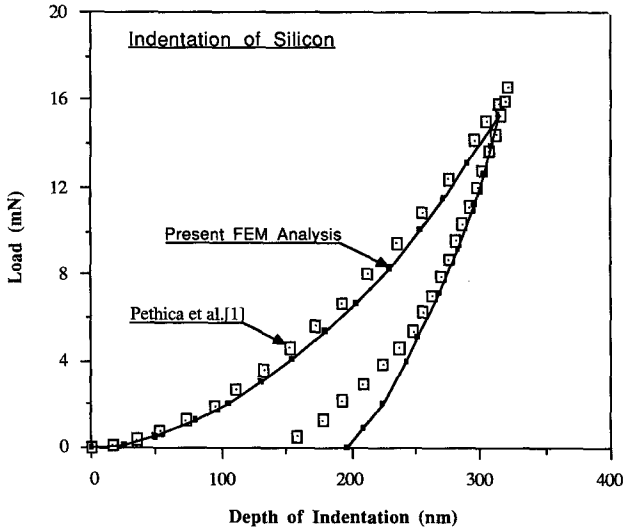

Fig. 4. Comparison between the results from the present FEM analysis and those from Pethica *et al.*[1] on indentation of silicon.

numerical and the experimental results may be due to differences in the actual and assumed yield stresses and work hardening rates of the materials involved. Also, the differences could be caused by differences between the tip geometry of the experimentally used indenter and the perfectly sharp indenter used in our calculations. The effect of tip geometry on the material response has been adequately discussed in Refs [1, 3].

Having shown that the finite element analysis can adequately describe the experimental load–displacement response, we next compute the hardness and Young's modulus from these simulations and compare the results with the material data used as input for the calculations. We have also analyzed two completely different types of materials; a low yield strength, high strain hardening material represented by aluminum and a very high yield strength, low strain hardening material represented by silicon. Elastic moduli for the two materials were also very different. Simulated results for these materials are given in Figs 5–7. Strain hardening was not included in the silicon simulation (Fig. 5). For indentation of aluminium, both cases of no strain hardening (Fig. 6) and full strain hardening (Fig. 7) have been considered. Prescribing linear strain hardening for silicon did not produce any

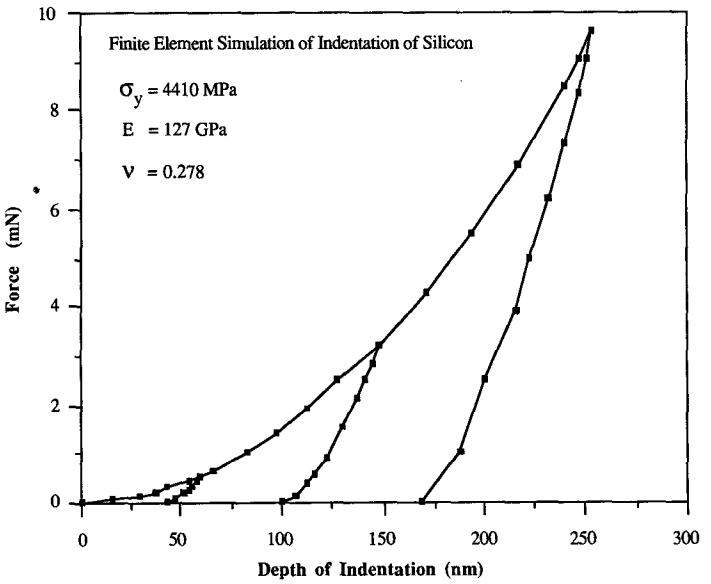

Fig. 5. Load–depth response for indentation of silicon.

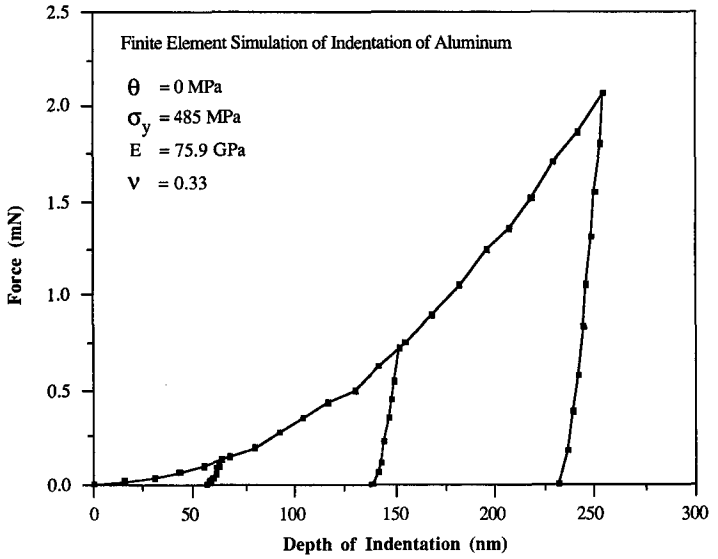

Fig. 6. Load–depth response of indentation of aluminum without strain hardening.

significant changes in the load–depth response. Unloading from three different points along the loading curve has been performed as shown. The general unloading response is similar to the experimentally observed response[1, 3]. As expected, silicon, with a high yield strength to elastic modulus ratio, shows a large amount of elastic recovery upon unloading whereas aluminum, with a low yield strength to elastic modulus ratio, shows little elastic recovery.

Hardness results

The microhardness is calculated as the load divided by projected area under the indenter at various points on the loading curve. These hardnesses are plotted as a function of indentation depth in Figs 8 and 9. The results show that the hardness is essentially independent of indentation depth. At smaller indentation depths, it was necessary to use a refined mesh size to obtain hardnesses that are independent of the depth of indentation over the range of depth considered. These results are expected for a homogeneous material described by a continuum based constitutive model. The calculations of hardness were performed using the load–depth results shown in Figs 5–7 and taking the value of contact areas directly from the FEM calculations.

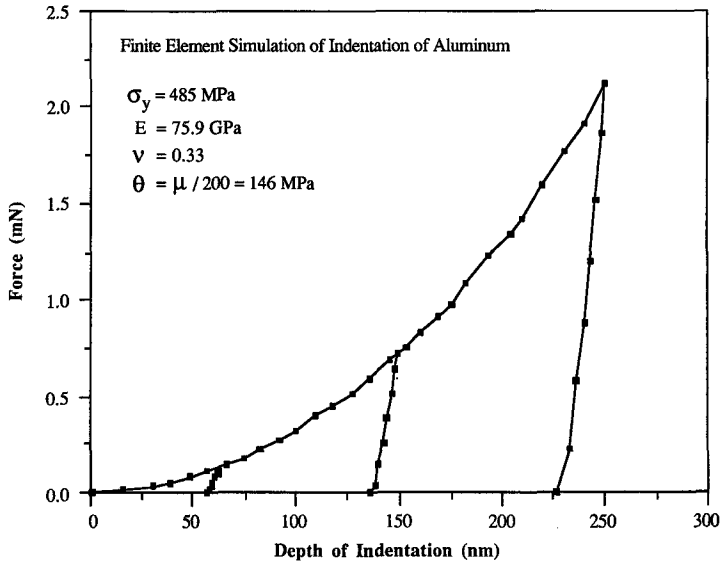

Fig. 7. Load–depth response for indentation of aluminum with strain hardening.

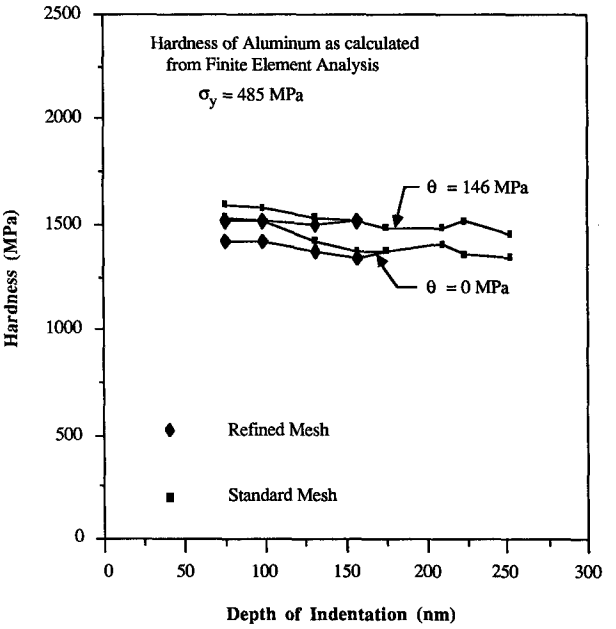

Fig. 8. Hardness variation as a function of depth of indentation for aluminum with and without strain hardening.

Determination of Young's modulus

As reported in Ref. [3], the slope of the unloading curve can be used as a measure of the elastic properties of the material being indented. If the contact area between the indenter and sample remains constant during initial unloading, the elastic behavior may be modelled as that of a flat ended cylindrical punch indenting an elastic solid. Loubet *et al.*[15] adopted the elastic solution given by Sneddon[16] and equated the projected area of contact with the indenter to the area of the punch. Obtaining an estimate of the true projected contact area under the indenter has been a source of some confusion because of the involvement of both elastic and plastic displacements under the indenter. The generally accepted procedure has been to estimate this contact area from the plastic depth of indentation. But, due to the elastic recovery of the indented material after unloading, the measured depth does not necessarily correspond to the plastic depth. It has been suggested[1] that for a

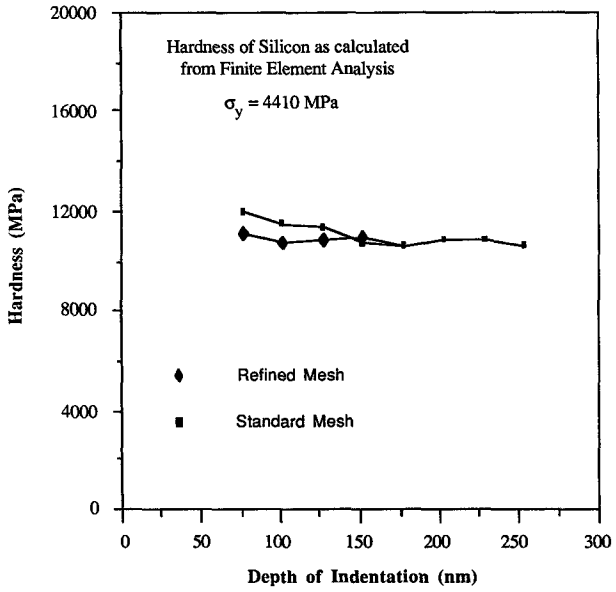

Fig. 9. Hardness variation as a function of depth of indentation for silicon.

material that exhibits a large amount of elastic recovery, the best estimate of the true, relaxed indentation depth is the depth at zero load, just before separation between the indenter and the material occurs. For a material that exhibits only a small amount of elastic recovery, the plastic depth can be taken as the depth at the highest load point, before unloading begins. An alternate suggestion in Ref. [3] is that the plastic depth for all materials is that point at which an extension of the linear unloading curve intersects the depth axis. These various possibilities for estimating the plastic depth and the corresponding contact area from the load–depth response are analyzed below.

Following the same analysis as proposed by Loubet *et al.*[15], but using the plastic depth, h_p, instead of the diagonal length used by them and assuming a perfectly rigid indenter with an ideal pyramidal geometry (having the same depth–area relationship as the Vicker's indenter), Ref. [3] obtained the following relationship for the elastic modulus:

$$E = \frac{(1-\nu^2)}{2h_p}\sqrt{\left(\frac{\pi}{24.5}\right)}\frac{dP}{dh} \tag{1}$$

where h_p is the plastic depth, dP/dh the slope of the unloading curve and E and ν are Young's modulus and Poisson's ratio, respectively. Below we use eqn (1) to estimate Young's modulus from the simulated load–depth curves.

The finite element results showed that for the first three points (on average) in the unloading curve, the indenter and the sample remained in contact. This suggests that it is valid to use eqn (1) to determine the elastic modulus of the specimen from the unloading slope. Because the contact area can be calculated directly from the FEM results, it is not necessary to use the plastic depth in determining the elastic modulus from the unloading slope. Rewriting eqn (1) in terms of the projected contact area, A, with the indenter, we obtain

$$E = \frac{(1-\nu^2)}{2}\sqrt{\left(\frac{\pi}{A}\right)}\frac{dP}{dh} \tag{2}$$

as an alternate expression for the elastic modulus.

With eqns (1) and (2) one can obtain the elastic modulus of the material being indented from the unloading slope dP/dh using either the plastic depth, h_p, or the projected contact area, A, with the indenter. As discussed above, the plastic depth may be determined from the intercept of the linear portion of the unloading curve on the depth axis or it may be taken to be either the depth at maximum load or the final depth in the unloaded state. As noted before, the projected contact area is found by knowing the radius of contact from the FEM calculations. To obtain a good estimate of dP/dh from the simulated load–displacement curves (Figs 5–7), a straight line was fit through the first three data points on the unloading curves. The highest load point at which the unloading begins was included in this fitting procedure. More points on the unloading curve with full contact between indenter and material could be obtained by using very small increments in displacement but at the expense of a large amount of computer time.

Table 2 summarizes various calculations of Young's modulus for aluminum and silicon using the methods described above. Out of the four calculated Young's modulus values, the first column involves the use of the flat punch model recast in terms of projected area of contact (eqn (2)) and the others involve the use of eqn (1). The second column makes use of the intercept of Ref. [3] to obtain the plastic depth. The third column is based on the assumption that the plastic depth is the final depth, i.e. the depth of indentation where the unloading curve reaches zero load value as proposed by Pethica *et al.*[1]. The fourth column involves the assumption that the plastic depth is the full depth of indentation at the point of maximum load. The purpose of these different types of calculations was to determine the effect of these various measures of plastic depth on the determination of Young's modulus. As seen from these calculations, the values of Young's modulus obtained using

Table 2. Comparison between theoretical and calculated values of Young's modulus

Depth of indentation (nm)	Calculated Young's modulus (GPa) Flat punch model	Extrapolated depth model	Final depth model	Full depth model
Material: silicon with no strain hardening (E = 127 GPa)				
254.0	131.0	121.0	143.2	96.4
152.4	123.6	121.4	137.2	89.1
61.8	126.9	120.8	137.3	88.9
Material: aluminum with no strain hardening (E = 75.9 GPa)				
247.08	77.2	72.2	74.0	68.3
151.05	76.9	71.0	72.4	66.1
61.65	76.8	71.6	73.2	65.4
Material: aluminum with full strain hardening (E = 75.9 GPa)				
252.38	77.8	72.9	73.9	67.3
149.52	77.2	71.7	74.7	67.4
61.65	76.8	71.4	72.0	65.4

the flat punch model coupled with the projected contact area from the FEM calculations (eqn (2)) are in very good agreement with the known values of Young's modulus for both materials. None of the methods based on plastic depth (eqn (1)) give equally good results. The extrapolated plastic depth model gives values that are near to but less than the known values of elastic modulus for both materials. Values of Young's modulus based on the final depth model are higher than the known value for silicon and less than the known value for aluminum. The full depth model gives values that are much less than the known values for both materials. Considering the results for both materials, the extrapolated depth model appears to give the best estimate of the projected contact area and the best procedure for determining the elastic modulus from loading and unloading curves alone.

Effect of elastic and plastic properties on hardness

So far we have not discussed the separate effects of elastic and plastic properties on the hardness of a material. Normally, the mean contact pressure under the indenter, p_m, is related to the yield stress of the material under compression, σ_y, by a generalized expression based on the deformation theory of a rigid–perfectly plastic solid[12] as

$$p_m = C\sigma_y \tag{3}$$

where C is a constant having a typical value close to 3. For ductile metals and other similar materials, this relationship works well. But, indentation experiments with highly elastic materials, such as polymers, have shown that the elastic and plastic strains associated with indentations are of the same order of magnitude and the above relationship does not apply. Johnson[13], using Marsh's[18] model of the expanding spherical cavity in an elastic–perfectly plastic solid derived a comprehensive relationship between the hardness, yield stress, Young's modulus and the indenter shape defined by the angle β between the indenter and the horizontal. For the case of an incompressible material, his results simplify to

$$\frac{H}{\sigma_y} = \frac{2}{3}\left[1+\ln\left(\frac{1}{3}\frac{E}{\sigma_y}\tan\beta\right)\right]. \tag{4}$$

He compared this prediction with experimental data for various kinds of materials and showed that for an indenter with a given geometry, the hardness of a material for an elastic–plastic material is not only a function of yield stress but also a function of the parameter E/σ_y, where E is the Young's modulus of the material.

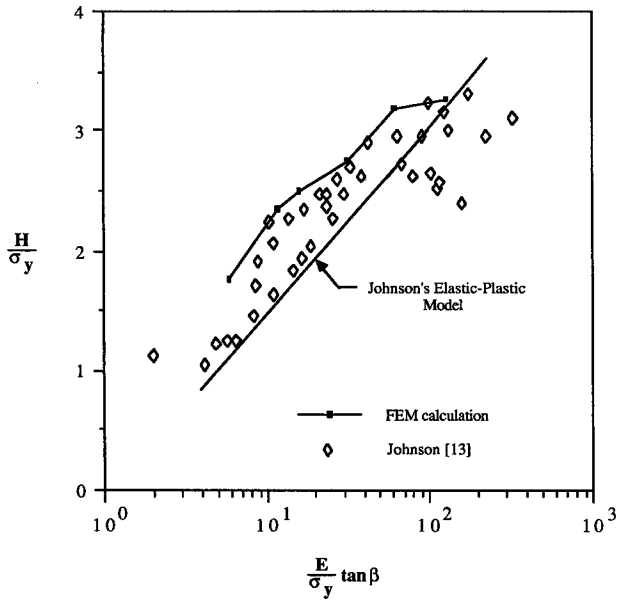

Fig. 10. Comparison of various experimental hardness results[13] with the predictions of Johnson's elastic–plastic model and the present FEM analysis.

In Fig. 10, we have compared the experimental data compiled by Johnson[13] with a few values of the hardness obtained from the present finite element analysis. Although the Johnson model correctly predicts the general trend in the data, it does not correlate the data well at larger values of E/σ_y where the data seem to reach a plateau, with H/σ_y values of about 3. This corresponds to the value predicted by rigid plastic theory from classical mechanics. The FEM analysis predicts an upper bound to the experimental results and also describes the plateau behavior at large values of E/σ_y. A more detailed analysis of the various predictions of the Johnson model is being made[19] and will be described elsewhere.

CONCLUSIONS

The results obtained from this study indicate that it is possible to successfully simulate the overall load–depth response of a sub-micrometer indentation test for different types of materials by using the finite element technique together with simple constitutive data as program inputs. It has also been demonstrated that one can obtain Young's modulus for the material from the slope of the linear portion of the unloading curve in such a simulation. This has been shown earlier in Ref. [3] and applied to actual test data. In addition, the FEM analysis yielded a hardness curve which was more or less independent of the depth of indentation. It is thus possible to obtain hardness values for the material from simulated data along the loading curve. The present study also gives theoretical justification for the use of the extrapolated depth as the best measure of the plastic depth of indentation. Finally, it has been shown that the FEM analysis predicts the response for an elastic–plastic material with respect to the relationship between hardness, yield stress and the Young's modulus of the material.

Acknowledgements—The authors wish to gratefully acknowledge the assistance of Dr M. F. Doerner of IBM in helping to formulate the problem herein. The authors are also grateful to D. Dungan of Center for Design Research at Stanford University for providing assistance in the use of their IBM 4341 computer system. The authors wish to thank the Defense Research Projects Agency for financial support through the University Research Initiative Program at UCSB under ONR contract N00014-86-K-0753.

REFERENCES

1. J. B. Pethica, R. Hutchings and W. C. Oliver, Hardness measurement at penetration depths as small as 20 nm. *Phil. Mag.* (*A*) **48,** 593 (1983).

2. N. Gane and J. M. Cox, The micro-hardness of metals at very low load. *Phil. Mag.* **22,** 881 (1970).
3. M. F. Doerner and W. D. Nix, A method of interpreting the data from depth-sensing indentation measurements. *J. Mater. Res.* **4,** 601 (1986).
4. S. Timoshenko and J. Goodier, *Theory of Elasticity*. McGraw-Hill, New York (1970).
5. W. Chen and P. Engel, Impact and contact stress analysis in multilayer media. *Int. J. Solids Structures* **8,** 1257 (1972).
6. R. B. King, Elastic analysis of some punch problems for a layered medium. *Int. J. Solids Structures* **23,** 1657 (1987).
7. R. J. Bourcier, C. M. Stone and F. G. Yost, A numerical and experimental study of the indentation hardness test. Sandia Report No. SAND 85-0486 (1985).
8. C. H. Lee, S. Masaki and S. Kobayashi, Analysis of ball indentation. *Int. J. Mech. Sci.* **14,** 417 (1972).
9. P. S. Follansbee and G. B. Sinclair, Quasi-static normal indentation of an elasto-plastic half-space by a rigid sphere—I. *Int. J. Solids Structures* **20,** 81 (1984).
10. C. Hardy, C. N. Baronet and G. V. Tordion, The elasto-plastic indentation of a half-space by a rigid sphere. *Int. J. Numer. Meth. Engng* **3,** 451 (1971).
11. A. G. Tangena and F. A. M. Hurkx, Calculations of mechanical stresses in electrical contact situations. *IEEE Transactions, Components, Hybrids and Manufacturing Technology*, Vol. CHMT-8, No. 1, pp. 13–20, March (1985).
12. D. Tabor, *The Hardness of Metals*. Clarendon Press, Oxford (1951).
13. K. L. Johnson, The correlation of indentation experiments. *J. Mech. Phys. Solids* **18,** 115 (1970).
14. C. Rubenstein, A critical appraisal of static hardness measurements. *J. Appl. Mech.* **48,** 796 (1981).
15. J. L. Loubet, J. M. Georges, J. M. Marchesini and G. Meille, Vicker's indentation curves of magnesium oxide (MgO). *J. Tribology* **106,** 43 (1984).
16. I. N. Sneddon, The relation between load and penetration in the axisymmetric Boussinesq problem for a punch of arbitrary profile. *Int. J. Engng Sci.* **3,** 47 (1965).
17. ABAQUS finite element program, HKS Inc., Providence, Rhode Island (1985).
18. D. M. Marsh, Plastic flow in glass. *Proc. R. Soc.* **A279,** 420 (1964).
19. A. K. Bhattacharya and W. D. Nix, Unpublished research.